Model-based feasibility assessment of a deep solar photobioreactor for microalgae culturing

Authors

M. Castrillo*, R. Díez-Montero and I.Tejero

*Corresponding author: M. Castrillo

Group of Environmental Engineering, Department of Water and Environmental Sciences and Technologies, University of Cantabria, Avda. Los Castros s/n, 39005, Santander, Spain.

Tel: (+34)942202293

Email address 1: castrillom@unican.es

Email address 2: ruben.diezmontero@unican.es

Email address 3: tejeroi@unican.es

Abstract

A deep photobioreactor (PBR) based on cone-shaped light guides was conceived to improve the solar light utilization efficiency of microalgae cultures, optimizing light distribution over the culture surface and thus minimizing photoinhibition and photosaturation occurrence. A preliminary model based on local light intensities and local growth rates was developed in order to check its viability. The model was applied to a conceptual PBR unit using irradiance data of Santander (Spain). Areal biomass productivities of 15.17 and 34.57 g m^{-2} d^{-1} were predicted for the most unfavorable and favorable months respectively, both under monthly average cloud cover. These results are, in average, 2.72 times higher than predicted values for an open pond PBR under identical irradiance conditions. A procedure to scale-up the deep

PBR in any location was developed. The procedure provides the optimal arrangement of the light guides and its operational parameters as a function of the surface incident light intensity. According to the obtained results, the novel configuration is highly efficient in land use, providing a low surface requirement solution.

Keywords: photobioreactor; microalgae; light utilization efficiency; light distribution; light guides; modeling

Abbreviations and symbols

A	Ground occupied surface of the PBR unit	m^2
Az	Azimuth angle	^{o}
b	Distance between the apex of the cone and the pivot joint	m
C	Cord of the base of the cone in the direction that they tilt	m
C_b	Culture biomass concentration	kg m^{-3}
D	Cone base diameter	m
F	Minimum distance between contiguous cones	m
F_β	Minimum distance between two contiguous cones in the direction of β	m
F_{N-S}	Minimum distance between two contiguous cones in the N-S direction	m
F_{W-E}	Minimum distance between two contiguous cones in the W-E direction	m
I	Direct light intensity over the cones' base	μE m^{-2} s^{-1}
I'	Direct light intensity over the internal surface of the cones	μE m^{-2} s^{-1}
I_l	Local light intensity in a point of the culture volume	μE m^{-2} s^{-1}
LPFD	Local Photon Flux Density	
K_a	Light extinction coefficient	m^2 kg^{-1}
K_i	Half-saturation constant	μE m^{-2} s^{-1}
n_1	Air refractive index	dimensionless

n_2	Cone's material refractive index	dimensionless
n_3	Culture suspension refractive index	dimensionless
L_{Rn}	Depth of the cone where reflected radiation hits	m
L_{Rn-1}	Depth of the cone where the previous reflection hits	m
q	Height of the cones above the water level to avoid splashing	m
Q	Height of the cones above the water level to avoid submersion	m
R	Reflected light	
S	Specular factor	%
S_I	Illuminated surface	m^2
S_I/V	Illuminated surface to volume ratio	$m^2\ m^{-3}$
T	Transmitted light	
Tr	Transmittance	%
Y_x	Biomass yield	(g biomass / mol PAR photons)
z	Distance between the wall of the cone and a point P(x,y)	m
α	Inclination angle of the cones to the horizontal, in any direction	^{o}
α_S	Maximum inclination angle of the cones in the South direction	^{o}
α_{min}	Maximum inclination angle of the cones in any direction	^{o}
β	Half of the rhombus angle in the grid formed by the cones	^{o}
μ_{max}	Maximum growth rate	d^{-1}
θ_i	incident angle	^{o}
θt	Refractive angle	^{o}
φ	Half aperture angle of the cones	^{o}

1. Introduction

In the last few decades the culture of microalgae has awakened scientific and commercial interest since these microorganisms have been seen as an attractive source of valuable biomass. A wide variety of applications have been attributed to algal biomass and its byproducts. Its utilization with environmental purposes like bioremediation and CO_2 fixation, as well as with commercial purposes in different industrial sectors, has been reported [1]. However its production at large scale is still limited. The cost of producing 1 kg of biomass in raceway ponds, tubular reactors and flat panels is estimated in 4.95, 4.15 and 5.96 € respectively (100 ha plants), which could be reduced to 1.28, 0.70 and 0.68 € kg biomass^{-1} by implementing improvements in the location, the mixing, the photosynthetic efficiency and the source of CO_2 and water [2]. A way to reduce its cost is to couple wastewater treatment based on microalgae with other purposes like biomass production for lipids extraction [3].

Microalgae are cultivated in production facilities called photobioreactors (PBR), which make use of light to produce biomass and byproducts. The design of large scale efficient PBRs is an issue that remains unsolved, mainly due to the nature of light that is attenuated while passing through the culture [4,5]. Illuminated surface to volume ratio (S_I/V) is a key parameter in PBR design, and with this idea a wide variety of devices, mainly consisting on narrow channels or panels, have been developed [6]. Nowadays there is a trend to reduce the reactors depth in order to increase light availability and therefore biomass productivity. It has been reported that reducing the water depth in raceways from 30 to 5 cm, can increase biomass productivity up to 72% [7]. However, reducing the water depth entails higher surface requirements.

On the way to find an effective utilization of light energy, systems that include internal light sources have been proposed. Also for scaling-up reasons, they are viewed as the only feasible configuration [8,9]. As conventional closed PBR, they are characterized by having a high S_I/V ratio, but additionally they allow for more compact designs [10]. Recently, PBR with internal

LED have been found as a suitable configuration with remarkable advantages like the possibility to scale-up in a three-dimensional way and to avoid overheating [11].

Considering solar light, an efficient utilization of the sunlight hitting the PBR surface is the key factor to achieve sustainable designs [12]. In a given geographical location, the amount of light that a culturing device receives is determined by the surface exposed to solar irradiance, therefore PBR must be designed to maximize its conversion efficiency. With this purpose, light harvesting and distributing methods have been proposed, especially by making use of Fresnel lenses and optical fibre [13-15]. More recently, systems driving the light deep into the reactor by means of vertical plastic light guides or empty chambers have been employed [16-18].

The use of solar light implies a big challenge in PBR design, since it is a non-scalable parameter that follows cyclical variations, but it is also affected by the weather and atmospheric conditions. In nutrient-limited systems, the limiting factor is a component of the medium, so it can be controlled by varying the dilution rate, but in light-limited systems, the limiting factor is not directly dependent on the dilution rate and cannot be assumed to be homogeneously distributed in the PBR volume [19]. Ideally, in a PBR the light inhibition and the complete dark zones should be avoided or at least minimized, keeping the light intensity between the critical and the saturation intensities. Then, the challenge consists on modulate the irradiance over the culture surface by varying its geometry or orientation in order to achieve a 'light dilution effect', with dilution factors ranging from 5 to 10 [20]. According to Posten, 2009 [21], the answer of process engineering is to design vertically mounted PBR with a large surface, where the sunlight falling on a given ground area is spread over a larger reactor surface. As a guidance value, it is reported that the surface to ground area ratio should be 10 or higher.

Solar tracking systems can help to achieve solar light capture optimization. Its use has been mainly applied to flat panels. It has been shown that using solar tracking systems enables a higher

irradiance in winter days by facing the panel perpendicular to the solar beams, thus increasing the overall productivity. On the contrary, at low cell densities or at high irradiances it is possible to provide lower irradiance over the culture by adjusting the tilt angle of the panel. According to the work of Hindersin et al., 2013 [22], the main advantages of using solar tracking systems are: (i) the possibility to decrease photoinhibition of photosynthesis in a microalgal culture of low density, by reducing the irradiance; (ii) enhancing the irradiance beyond 100 % of the horizontal irradiance in high cell density cultures by exposure of the reactor perpendicular to the sun light and (iii) regulating culture temperature by adjusting the irradiance or cooling to avoid heat stress.

Large scale PBR optimization and modelling is governed by two main types of phenomena: on the one hand the biokinetics of the species to be cultured, and on the other hand the PBR physical structure that determines the radiant light transport. At the same time, when designing a solar based PBR, two main types of factors must be taken into account. Firstly, the shape and geometry of the PBR, like its exposed surface and the presence of shadowing elements, and secondly geographical factors like the latitude and the relative position of the Sun. In non-sun tracking PBR, direct irradiance over the reactor surface depends on the incident angle, which depends on the solar position. However, sun tracking PBR are usually designed to receive the optimal radiation over the time, thus their geometry and dimensions must be designed and calculated according to the different positions of the Sun from the sunrise to the sunset through the year. Since daily Sun path varies along the year, especially in high latitudes, the optimized design must satisfy the global maximum productivity, thus averaged irradiance values should be avoided.

Knowing the angle of incidence of the direct light beams all over the day becomes essential to calculate light gradients inside the culture and to avoid heterogeneously irradiated surfaces. The study of the tilt angle for optimal year-round energy collection and, when possible, the adjustment of this angle through the year has been recognized to result in an enhancement of the overall annual productivity [23,24].

Many approaches can be found in scientific literature to model volumetric or areal productivity of microalgae. As a first classification, two border cases can be distinguished: models that predict the photosynthetic activity according to the local conditions of a cell at a given position inside the PBR and models that use averaged parameters. Secondly, within each group, the light dependence can be calculated in different ways although the most common approach is to consider that light dependence follows Monod-type kinetics. Among the models that use averaged parameters, the most basic approach is to consider the light intensity in the PBR as the average of all the local intensities within the same. The average irradiance can be defined as the irradiance experienced by a single cell randomly moving inside the culture [25]. However, average irradiance is not a sufficient criterion of culture performance because it considers only the total length of the dark and the light periods, not their frequency and reactors presenting identical averaged irradiances can show different productivity [10,26], so more sophisticated models have been developed based on averaged parameters, as it is reported below.

Yun et al. [27] compared four different models: two models based on local conditions and two other ones using averaged-parameters. Within each type, the light dependence can be expressed as a function of the photon flux density or the photon absorption rate. According to their results, the models based on local conditions could predict the experimental data more accurately.

Bosma et al. [28] compared a no–light integration and a full–light integration model, based on photosynthetic yields, both using local photon fluxes. The first case assumes that microalgae that move through the light gradient are able to adapt immediately to the new conditions, then photosynthetic yields can be calculated with local light intensities. On the contrary, the fully-integrated approach assumes that acclimation processes occur slower than the light/dark cycles in the photobiorreactor, which means that the cells are adapted to the average light intensity, thus photosynthetic yields are dependent on the average intensity. According to the work of Bosma et al., 2007, the light integration approach over-predicts the productivity since in this model no

photoinhibition can occur. In contrast, the no–light integrated approach under–predicts the productivity because it over–estimates the photoinhibition and photolimitation processes.

In this work the feasibility of a deep PBR (Patent Number WO2012072837 A1) [29] conceived to take advantage of the irradiance falling over its surface is assessed. A Local Photon Flux Density (LPFD) model [27] was applied to a unit of volume of the PBR. This model approach is useful to assess the sensitivity of the productivity to the geometry of the reactor as well as to the culture conditions. The scale-up of this PBR would be performed by repeating identical units, but the relative position of the PBR units must be carefully decided in order to allow for a maximum light harvesting. Therefore, a procedure to define the cones arrangement in order to maximize the light capture when scaling-up this PBR was also developed. The procedure is also useful to prospect for potential locations of this PBR.

2. Materials and methods

2.1. Description of the photobioreactor

The hereby presented configuration consists on a tank including a series of conical structures made of a transparent material, such as plastic, which are submerged in the bulk culture medium, with the base placed in the upper side over the water surface (Figure 1). A sun tracking system allows the cones to be positioned with its base in a plane perpendicular to the direct incident solar light beams. These conical structures guide the light downward since they receive the incident solar light on their base and spread it out through its lateral surface. The full scale tank dimensions result from the repetition of the conical structures and its surrounding culture volume, which means that the tank does not need to have a specific shape and existing tanks could be reused for this purpose. On the contrary to conventional columns or panel photobioreactors, there are no vertical structures over the ground, so shading phenomenon is eliminated and there is no need for separation between reactors or reactor units to scale-up. The tank is fully mixed thanks to air (or

CO_2-enriched air) bubbling and, if needed, submerged stirrers. More details regarding the full scale implementation of this invention can be checked in the patent document [29]. The configuration was experimentally tested indoor at bench-scale [30], but in order to explore its maximal performance and optimize its design using solar light, the photosynthetic activity as a function of operating conditions and reactor geometry is hereby modeled.

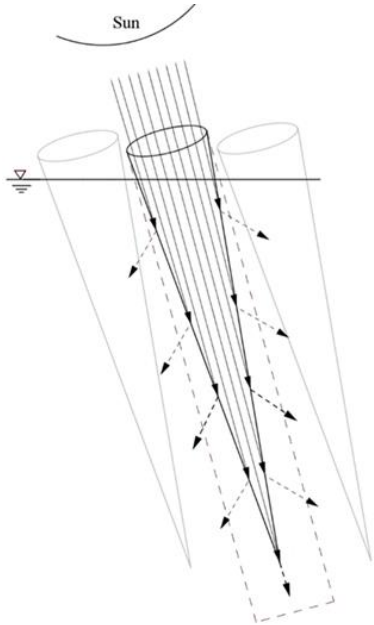

Figure 1. Scheme of the conceptual PBR. Continuous arrows represent incident radiation while dotted arrows represent refracted radiation.

2.2. Photobioreactor design criteria

The design of this PBR was mainly based on a light distribution criterion, with the basic premise of using solar light, although the device is adaptable for artificial light. Furthermore, the need for maintaining the culture properly mixed and the easiness to scale-up are factors that were present during the conception of the idea. A PBR that can be scaled-up as a repetition of units is desirable, being one unit a single light distributing device and the surrounding culture [8]. At a given light intensity there is an optimum unit size, and this should be theoretically or experimentally determined.

As mentioned before, the reactor consists on a deep tank (between 1 and 2 meters) that contains the microalgae culture, in which a number of transparent conical structures are submerged or semi-submerged, with their apex towards the bottom of the reactor, to drive the light all along the depth of the tank. These structures are orientated by means of a solar tracking system to follow the direct solar radiation. As shown in Figure 2, the light distribution surface (cones' lateral surface (dS')) is larger than the light receiving surface (cones' base (dS)). As a result, the irradiance over the culture surface is attenuated with respect to a horizontal one, reducing the photoinhibition phenomenon occurrence and enhancing the illuminated surface-to-volume ratio. Once the optimum reactor unit characteristics are determined, the photobioreactor could be scaled-up by increasing the number of reactor units [8].

The geometry of a cone was found to meet the criteria of distributing the light uniformly and modulate the light intensity to provide the desired values to the culture, preventing from photoinhibition and photosaturation. While other geometries like a tube would result in a high irradiance on the bottom and only diffuse irradiance over the lateral walls, the conical shape allows for a homogeneous irradiance which, in addition, can be modulated during the design process in accordance to the specific needs of the culture and the irradiance of the geographical area where the PBR is going to be installed.

The irradiance over a surface takes its maximum value when this surface is perpendicular to the solar beams. As the tilt angle of the surface is higher, the irradiance decreases, as it is stated by Lambert's cosine law. For a cone with an aperture angle of 2φ, the irradiance over the internal face of the cone (I') is calculated as in Eq.1, where I is the irradiance over the base of the cone (perpendicular to the solar beams).

$$I' = I \times \cos(90 - \varphi) \qquad \text{Eq.1}$$

This means that the irradiance over the culture for a given geographical area can be modulated by determining the aperture of the cone.

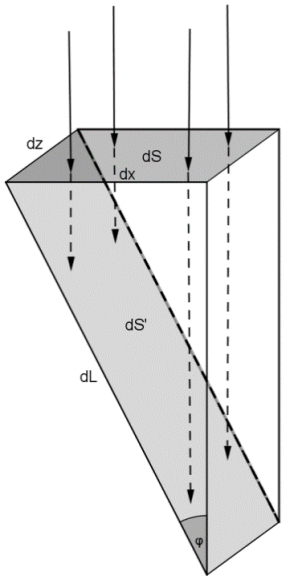

Figure 2. Representation of the solar beams incidence over the lateral wall (dS') of a cone with aperture angle 2φ.

2.3. Description of the model

2.3.1. Three-dimensional problem domain

In order to model the biomass productivity in the PBR, the solution was approximated by the finite element method. The domain of the problem was defined as a unit of volume of the PBR, which is the minimum unit that would be repeated when scaling-up this technology. This unit consists on a right circular fictitious cylinder with a right circular cone inside. The base of the cone coincides with the upper base of the cylinder and its apex points to the lower base of the cylinder. The domain of the problem is the volume that remains between the cylinder and the cone. For this first approach to assess the biomass productivity, spaces between contiguous cones receiving direct radiation, were considered negligible with respect to the total illuminated surface.

The aperture of the cone (2φ) was used to calculate light falling over the reactor surface from irradiance over the cone's base. According to the reflected irradiance over the inner surface of the

cone, several subdomains were defined. The determination of their boundary conditions is described in the following section.

Representing the longitudinal section of the PBR unit in a two-dimensional Cartesian coordinate system, with the abscissa axis orientated in the direction of the base of the cone and the ordinate axis parallel to the longitudinal axis of the cone, the position of a point P can be described according to its coordinates *x* and *y* at a distance *z* to the lateral surface of the cone. The whole domain was discretized on a mesh composed by 1cm * 1cm squares with their faces *dx* and *dy* parallel to the abscissa and ordinate axis respectively. Since the irradiance reaching a point P of the culture depends on its distance to the irradiated surface, which is the inner surface of the cone, homogeneously illuminated ring shaped volume units can be differentiated around the cone with its cross-section being an element of the mesh, as represented in Figure 3.

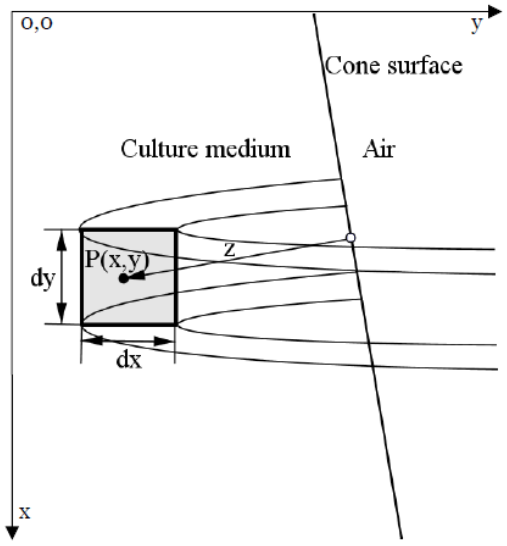

Figure 3. Homogeneously illuminated ring shaped volume with section dx*dy and a point P(x,y) in the center of this section.

In order to compare the obtained results with a conventional well-known technology, the same calculation scheme was applied to an open pond with the same ground surface occupancy. Different depths of the open pond were tested and 0.2 m was chosen since it was the one that

provided the best results. In the case of the open pond the domain is the whole volume of the tank because the whole tank contains culture medium while in the innovative PBR only the portion between the cone and the fictitious cylinder contains culture medium. Variables and constants were identical in both cases.

2.3.2. Incident light

The total irradiance received by a surface on the Earth is the addition of the direct radiation, the diffuse radiation and the reflected radiation. Direct radiation arrives to the Earth's surface without having varied its direction. In the case of the cone, the direct irradiance received over its inner surface is homogeneous and its value is the irradiance of the geographical place over a two-axis tracking system but applying the Lambert's cosine law. In the case of the open pond, the incident irradiance is the irradiance over a horizontal surface. Diffuse radiation arrives to the Earth's surface after having varied its direction during its path through the atmosphere due to scattering. While direct radiation has a definite direction, diffuse radiation may come from any direction. Finally, reflected radiation is defined as that that hits some object and is reflected arriving to the object of interest. PBR are usually considered to be away from where the reflected light can arrive, so reflected radiation rarely accounts for a significant part of the sunlight striking their surface. However, in the present case, the direct radiation received by the inner surface of the cones is not totally transmitted to the culture; some portion can be reflected and fall over another part of the cone. According to the Fresnel equations the fraction of light that is transmitted (T) and the fraction that is reflected (R) depend on the angle that the incident beams make to the normal (θ_i) and the refractive index of the object (n). Due to the shape of the cones, the reflected radiation is redirected to the bottom of the cones, so losses by reflection are minimized thanks to the shape of the cone and most of the cone's surface receives homogeneous radiation. Furthermore, since reflected radiation is directed towards the bottom of the cone, higher irradiance arrives to the

deepest zone of the reactor, where normally the darkest conditions are found. In the case of the pond, a fraction of light is reflected and lost.

Considering that the incident light is unpolarised, R can be calculated as in Eq.2, where R_S is the reflectance of an incident light beam that is polarized with its electric field perpendicular to the plane containing the incident, reflected, and refracted beams and R_P is the reflectance of an incident light beam that is polarized with its electric field parallel to the plane described above. T is calculated as in Eq.3.

$$R = \frac{R_S + R_P}{2} \quad \text{Eq. 2}$$

$$T = 1 - R \quad \text{Eq. 3}$$

R_S and R_P are calculated by means of the Fresnel equations (Eq.4 and Eq.5), where n_1 and n_2 are the refractive indexes of media 1 and media 2 respectively, θi is the angle that the incident beams make to the normal and θt is the angle that the refracted angle makes to the normal direction.

$$R_S = \left(\frac{n_1 \cdot \cos\theta_i - n_2 \cdot \cos\theta_t}{n_1 \cdot \cos\theta_i + n_2 \cdot \cos\theta_t}\right)^2 \quad \text{Eq. 4}$$

$$R_P = \left(\frac{n_1 \cdot \cos\theta_t - n_2 \cdot \cos\theta_i}{n_1 \cdot \cos\theta_t + n_2 \cdot \cos\theta_i}\right)^2 \quad \text{Eq. 5}$$

θt is calculated by means of Snell's Law:

$$\frac{n_1}{n_2} = \frac{\sin\theta_t}{\sin\theta_i} \quad \text{Eq. 6}$$

The cones are made of a transparent or translucent material which is characterized by its transmittance (T_r). Finally, the cone's material has been considered as a mixed specular-diffuse reflector, thus a Specular Factor (S) has been attributed to it, representing the fraction of light that is reflected as specular light, while the rest is reflected as diffuse light.

Taking into account the geometrical and trigonometrical relations between the shape of the cone and the reflected beams direction, the depth of the cone where reflected radiation hits (L_R) can be calculated as in Eq.7, where D is the diameter of the cone and φ is half of the aperture angle of the cone.

$$L_R = \frac{D}{(\cos\varphi)(\tan 2\varphi + \tan\varphi)} \quad \text{Eq. 7}$$

Depending on the depth of the cone and its aperture angle, successive reflections can be produced, reaching a depth ($L_{R(n)}$) that is calculated like L_R but taking into account the relation between D and the diameter of the cone at the height of the previous reflection ($L_{R(n-1)}$), as presented in Eq.8.

$$L_{R(n)} = \frac{D - 2(L_{R(n-1)} \sin\varphi)}{(\cos\varphi)(\tan 2n\varphi + \tan\varphi)} + L_{R(n-1)} \quad \text{Eq. 8}$$

Due to the reflections, different depths of the cone receive different irradiance, demarcating the sub-domains of the problem. A height of 0.20 m was kept between the apex of the cone and the bottom of the cylinder.

In the case of diffuse radiation, it is considered to be homogeneously distributed over the whole cones inner surface and that it is attenuated along the distance *z*.

Irradiance data were obtained from the Photovoltaic Geographical Information System (PVGIS) [31]. The database provides irradiance data for real-sky conditions on a 2-axis tracking plane and on a horizontal surface throughout an average day of each month, as well as the ratio diffuse to global irradiation for a given geographical area. Real-sky conditions mean that data are calculated taking into account average cloud cover for each month. Data are provided for 15 minutes intervals along the day.

Irradiance data in the area of Santander (Spain, 43°27'44" North, 3°48'35" West, Elevation: 16 m a.s.l.) were taken as input data for the present model (Appendix Section 1). It was considered that

Photosynthetic Active Radiation (PAR) accounts for approximately 45% of the total incident radiation.

2.3.3. Light gradients

As the model assumes that microalgae growth directly depends on local light intensity, knowing the fraction of light that arrives at any point of the culture is needed. The irradiance at any point of the culture depends on:

- the total incident radiation at the surface of the culture
- the optical properties of the culture
- the distance between that point and the irradiated surface.

Once the irradiance over the cone surface is known as the addition of direct radiation, diffuse radiation and reflected radiation, in order to predict the light intensity at any distance of the irradiated surface, Lambert-Beer Law is the most widely applied expression (Eq.9), where I_l is the local light intensity (μE m^{-2} s^{-1}) at a point situated at a distance z (m) from the irradiated surface, I' is the received light intensity over the irradiated surface of PBR (μE m^{-2} s^{-1}), K_a (m^2 kg^{-1}) is the extinction coefficient and C_b (kg m^{-3}) is the biomass concentration. K_a was experimentally determined as shown in the Appendix (Section 2). The result was 182 m^2 kg^{-1}.

$$I_l = I' e^{-K_a C_b z} \quad \text{Eq. 9}$$

Although more complex expressions have been developed [32] in order to consider the light spreading by the solid particles, this phenomenon is usually negligible compared to the absorption by the biomass. Furthermore, when the extinction coefficient is experimentally determined, all these phenomena are directly affecting the measure, so they are already included in such coefficient.

In the case of the direct radiation, the light path between the cone's surface and the point *P(x,y)* is usually calculated according to the Sun position [33,34]. However, since in the case of the present reactor the cones tilt according to the Sun position in such a way that the direct radiation is always perpendicular to the cones base, the light path does not depend on the position of the Sun. Light has been considered to be scattered once it reaches the culture suspension, being converted in diffuse radiation. Although a theoretic refraction angle has been calculated to know the fraction of refracted and transmitted radiation, in order to calculate the attenuation of light as it goes through the culture, the distance in the direction perpendicular to the cones lateral wall (z) has been considered instead of z_{direct}, which would be the path that an ideal direct beam would take.

According to the coordinates *x* and *y* of the point *P* within the modelled domain, its distance to the irradiated surface can be calculated as in Eq.10.

$$Z = [(y \tan \varphi) - x] \cos \varphi \qquad \text{Eq. 10}$$

By substituting Eq.10 in Eq.9, the light intensity at a given point can be expressed as a function of its position *P(x,y)*.

2.3.4. Local growth rate

The model assumes that the reactor is fully mixed and that cells experiment a growth rate dependent on the LPFD [27]. The kinetic expression determines the specific production inside a bioreactor system as a function of the limiting factor. In light-limited cultures, the Monod-type model is a general kinetic model for describing the relationship between an organism growth and the concentration of the limiting factor, which in this case is the light. The use of this equation (Eq.11) is valid when the light intensity inside the PBR is under inhibitory levels.

$$\mu = \frac{\mu_{max} I_l}{K_s + I_l} \qquad \text{Eq. 11}$$

In Eq.11, μ_{max} is the maximum specific growth rate (d^{-1}), K_s is the half-saturation constant ($\mu E\ m^{-2}s^{-1}$) and I_l is the local light intensity. The kinetic parameters were experimentally determined (procedure shown in Appendix Section 3). The results were μ_{max}=1.02 d^{-1} and K_i=42.45 $\mu E\ m^{-2}s^{-1}$.

2.3.5. Overall productivity

Overall productivity in the PBR unit can be calculated by integrating the productivity of the ring shaped homogeneous volumes (dV). In the case of the pond, homogeneously illuminated volumes are horizontal layers parallel to the reactor surface.

The overall productivity as grams of biomass per square meter and day can be calculated as in Eq.12.

$$P = \frac{\sum(\mu_i\ dV\ C_b)}{A} \qquad \text{Eq. 12}$$

Being μ_i the local growth rate (d^{-1}), dV the volume of a homogeneously illuminated volume (m^3), C_b the biomass concentration ($kg\ m^{-3}$) and A the ground occupied surface of the PBR unit (m^2).

The variables and constants of the biomass productivity model are sum-up in Table 1.

Variables		
Name	**Abbreviation**	**Unit**
Half of the aperture angle	φ	°
Cone base diameter	D	m
Culture concentration	C_b	$kg\ m^{-3}$
Constants		
Name	**Abbreviation**	**Unit**
Light extinction coefficient	K_a	$m^2\ kg^{-1}$
Maximum growth rate	μ_{max}	d^{-1}
Half-saturation constant	K_i	$\mu E\ m^{-2}s^{-1}$
Air refractive index	n_1	-
Cone's material refractive index	n_2	-
Culture suspension refractive index	n_3	-
Transmittance	Tr	-
Specular factor	S	-
% PAR within global radiation	% PAR	-

Table 1. Variables and constants of the model

2.3.6. Photosynthetic efficiency and biomass yield

Considering that photosynthesis needs 8 moles quanta to produce 30 grams of biomass (as $C_6H_{12}O_6$), the maximum biomass productivity was calculated according to the irradiance data in Santander. Then the photosynthetic efficiency could be calculated as the percentage of biomass produced in the PBR unit in relation to the maximum theoretical productivity, which was calculated according to the irradiance over a two-axis tracking system in both –the novel PBR and the open pond– cases.

$$\text{Photosynthetic efficiency (\%)} = \frac{\text{Estimated biomass productivity (g biomass m}^{-2}\text{d}^{-1})}{\text{Maximum theoretical biomass productivity (g biomass m}^{-2}\text{d}^{-1})} \times 100 \quad \text{Eq. 13}$$

The biomass yield (Y_x) on a PAR basis was calculated as in Eq.14.

$$Y_{x=} \frac{\text{Estimated biomass productivity (g biomass m}^{-2}\text{d}^{-1})}{\text{PAR photons (mol m}^{-2}\text{d}^{-1})} \quad \text{Eq. 14}$$

2.3.7. PBR scale-up

A procedure to define the optimal arrangement of the cones in the PBR when it is scaled-up was carried out by modelling the working illuminated volume of a PBR unit through the year. The amount of light that a single cone receives depends on the angle (α) to which it can tilt with respect to the horizontal for each Azimuth (Az). The more the cones can tilt, the longer through the day they will receive direct light. In addition, the more cones, the more light will be distributed by the cones instead of falling directly over the horizontal surface of the culture. However, the angles α to which the cones can tilt depend on the distance between the cone and the adjacent ones. Therefore, an optimum distance between adjacent cones must be found to provide the highest illuminated volume to occupied surface ratio over the year. In this study, it has been considered that Az=0º in the South direction, while East and West have Az = 90° and north 180°. The arrangement of the cones makes a grid whose nodes are the center of the base of the cones when they are vertically placed. The rhombus comprised among four nodes is characterized by the length of its side (F_β), which is the distance between two contiguous cones, and its angle, which is twice the angle between a side of the rhombus and the South (β) (Figure 4).

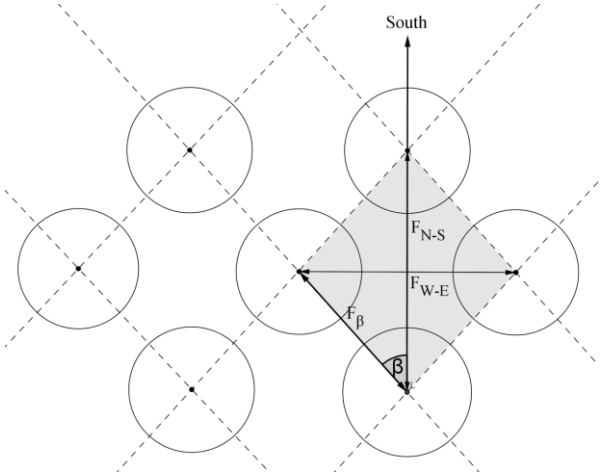

Figure 4. Top view of the cones distribution in the PBR with the South direction as reference.

Once the diameter and the aperture angle of the cones have been optimized according to the previously described model, there are three input variables that allow for the evaluation of the direct irradiance that an arrangement allows to distribute. It is considered as captured irradiance, the direct light entering into the cones perpendicularly to its base plus the diffuse radiation. The number of hours through the year that the cones are receiving direct radiation and the illuminated volume that they provide are also calculated. The three input variables are:

The pivot joint distance to the apex of the cone (b): The cones, acting as light distributors, are placed with its base in the upper side and its apex towards the bottom. However, the base cannot be placed at the water line level, since a minimum height (q) above the water level must be fixed in order to avoid splashing over the cone's base. Furthermore, the cones base has to stand out above this fictitious line not only when they are in vertical position, but also when they tilt in order to track the Sun, then an additional height must be added (*Q*). The cone inclination takes place over a pivot joint, which is located in a fixed point situated along the central axis of the cone. If the pivot joint is located in the base, the value of *b* will be the height of the cone, taking into account the value of *q* and *Q*. On the contrary, if the pivot joint is in the apex, the value of *b* will be 0.

As a cone tilts from vertical position, the submerged fraction of the cone varies and therefore the water level rises or falls when the submerged volume decreases or increases respectively. In the case of the pivot joint in the base, the submerged volume firstly increases but from a certain angle it lowers because the part of the cone that stands out above the water is bigger than initially was, thus the water level decreases. In the case of the pivot joint in the apex the submerged volume always increases as the cone tilts, thus the water level always rises. *Q* is optimized by adjusting its value to make the distance between the base and the water level the minimum possible when the cones are tilted to its maximum angle and it depends on the situation of the pivot joint.

In Figure 5 the two border cases are represented: the pivot joint in the base and the pivot joint in the apex. The deeper is the situation of the pivot joint (the nearer to the apex), the longer must be the distance between the cone base and the water level to tilt the same angle, thus the base is larger. As an example, in Figure 5 both cones have been tilted to $\alpha=60^{\circ}$, and both have the same submerged volume when they are in vertical position (the shading part). The one that has the pivot joint in the apex has a higher part over the water level –*Q*–, resulting in a higher consumption of material for the construction of the cones and in a higher separation between adjacent cones. In contrast, since the apex remains static, the deep reached by the light is constant

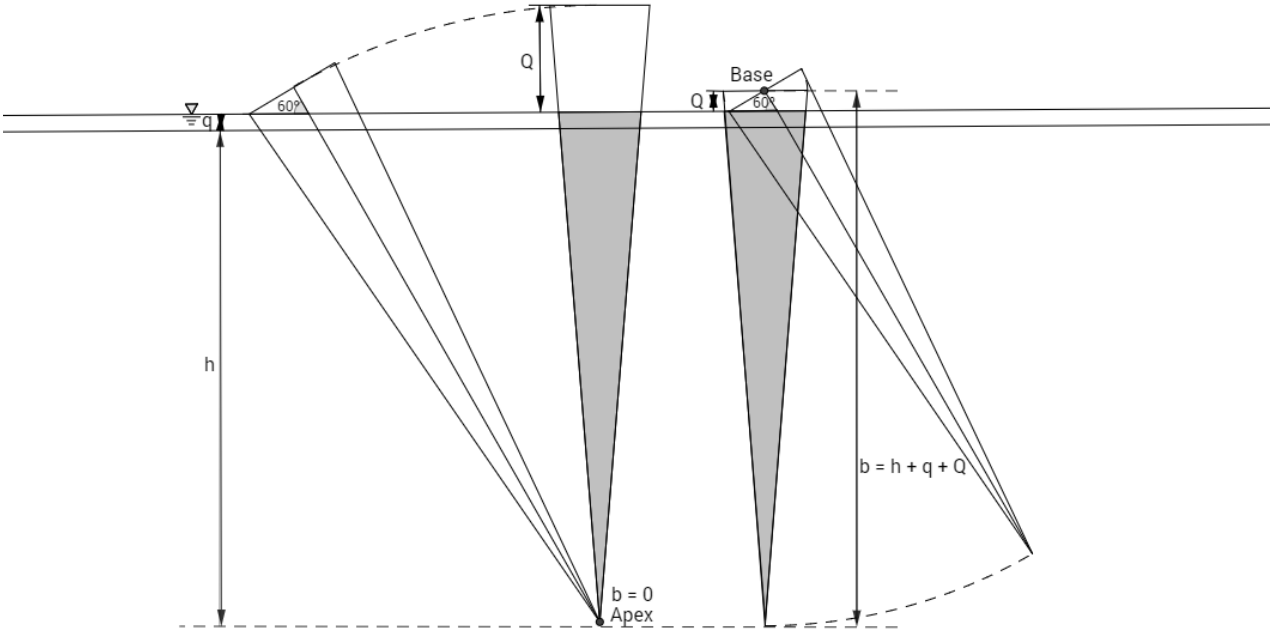

Figure 5. Scheme of the two extreme cases of situation of the pivot joint: in the apex and in the base. In both cases the cones are inclined to α=60º.

Maximum inclination angle in the South direction (α_S): This variable allows for the calculation of the N-S diagonal of the rhombus of the grid, in other words the distance ($F_{N\text{-}S}$) from one cone and the adjacent one in the South direction.

The minimum distance (F) between adjacent cones is determined from the minimum α that the cones can take in that direction (α_{min}), which is also related to the base diameter through *Q*. This distance can be calculated as indicated in Eq.15, where C is the chord of the base that gets in touch with the contiguous cone in the Az direction. Geometrically, C is the chord of a base that is formed by a segment with Az direction that pass through the half point of F_β. When the cones tilt in N-S, W-E or β direction, C takes the value of the diameter of the cone. When $\alpha=\alpha_S$, then $F=F_{N\text{-}S}$. The scheme of the cones with the dimensions C and D and its relation with F are graphically represented in Figure 6.

$$F = C\left[\text{sen}\,\alpha + \frac{\cos\alpha}{\tan(\varphi+\alpha)}\right] \qquad \text{Eq. 15}$$

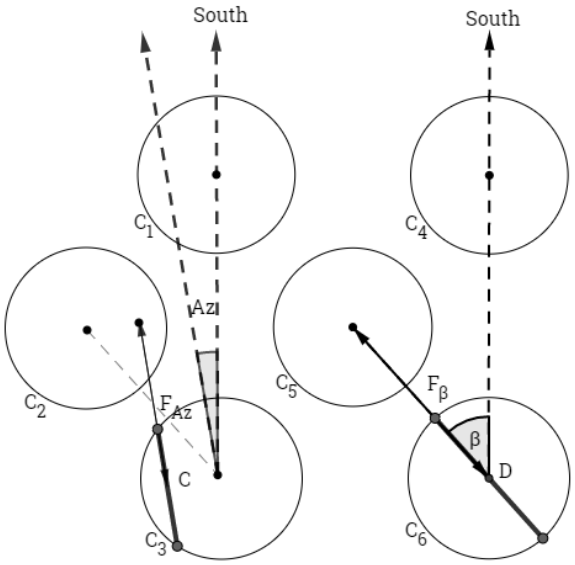

Figure 6. Top view of the cones and scheme of the relations between F, C and D. C1, C2 and C3 tilt in Az direction. while C4, C5 and C6 tilt in β direction.

The angles α for each Az through the year coincides with the solar elevation angle, and have been calculated from the latitude, the earth declination and the hour angle (procedure shown in the Appendix Section 4).

Half of the rhombus angle (β): This parameter together with α_S allows for the determination of the grid dimensions. Once the diagonal in South direction is known ($F_{N\text{-}S}$), the distance from one cone and the contiguous cone in β direction (F_β) can be calculated as in Eq.16.

$$F_\beta = \frac{\frac{\overline{F_{N-S}}}{2}}{\cos\beta} \qquad \text{Eq. 16}$$

Finally, the distance between one cone and the contiguous one in the East direction ($F_{W\text{-}E}$) is calculated as in Eq.17.

$$F_{W-E} = F_{N-S}\tan\beta \qquad \text{Eq. 17}$$

The resolution of the equations above gives two main results for each distribution: the number of cones per unit surface and the maximum tilt angle for each Az angle, which at the same time determines the irradiance captured by the cones.

Finally, in order to evaluate the distribution efficiency, the illuminated working volume per unit surface was calculated. The illuminated working volume has been defined as the culture volume that receives an intensity of light between the compensation point for photosynthesis and the saturation point. Then the working illuminated volume is considered as a margin that surrounds the submerged fraction of the cone in each moment. The width of this margin can be determined according to the previous model as a function of the biomass concentration and the light extinction coefficient of the species to be cultured. As explained before, the volume of the cone, and therefore the volume of the illuminated margin of the cone, that remains submerged for each inclination angle can be calculated. Therefore, the comparison variable for the different distributions is the working illuminated volume multiplied by the time during which this volume is maintained, per unit surface and per year (m3 min m-2 year-1).

The variables and constants of the cones distribution model are sum-up in Table 2.

Variables		
Name	**Abbreviation**	**Unit**
Half of the aperture angle	φ	°
Cone base diameter	D	m
Pivot joint distance to the apex of the cone	b	m
Inclination angle (Az=0º)	α_S	°
Half of the rhombus angle	β	°
Constants		
Height of the cones above the water level to avoid splashing	q	m
Other parameters		
Height of the cones above the water level to avoid submersion	Q	m

Table 2. Variables and constants of the model

3. Results and discussion

3.1. Cone geometry and biomass concentration setting

Considering that light is the only limiting factor in the culture, there are several decision variables that influence volumetric and areal biomass productivity. Relating the geometry of the PBR unit, the diameter of the cone as well as the aperture angle of the cone affects the areal productivity of the PBR, since they determine the angle of the irradiated surface and the depth and occupied ground area of a unit. The largest is the base of the cone, the deeper can be the reactor but a higher distance must be maintained between two cones in order to avoid them to touch each other when they are inclined, making dark areas larger. Furthermore, there will be fewer units per unit surface. Small dark areas are desirable in order to increase the light-dark cycles frequency.

According to the growth kinetics parameters of *S. obliquus*, to maintain the light intensity in the upper layers of the culture under saturation values, the aperture angle must be around 10º (φ=5º). According to the Fresnel equations, in each reflection 61% of the incident light is transmitted to the culture while 39% is reflected.

For a certain aperture angle, the higher is the diameter of the cone, the lower is the illuminated surface to culture volume ratio. However, since the distance of the light path remains constant, above the optimal cone's base diameter the illuminated volume to the dark volume ratio decreases and below the optimal cone's base diameter the light path is restricted to the limits of the fictitious cylinder that contains the culture. 0.30 m has been seen as the optimal diameter for a sole PBR unit. In a geometry with D=0.30 m and φ=5º, the farthest point to the irradiated surface keep a distance of 149 mm to it.

The dimensions and characteristics of the modelled PBR unit and an open pond with the same ground surface occupancy are summarized in the Table 3.

Parameter	Unit	PBR	Open pond
PBR unit diameter	m	0.3	0.3
Cone diameter	m	0.3	-
Cone height	m	1.63	-
PBR unit height	m	1.83	0.3
Occupied surface	m^2	0.07	0.07
Culture volume	m^3	0.09	0.021

Illuminated surface to occupied surface ratio	$m^2\ m^{-3}$	11	1
Occupied surface to culture volume ratio	$m^2\ m^{-3}$	0.78	3.33
Illuminated surface to culture volume ratio	$m^2\ m^{-3}$	8.41	3.33

Table 3. Main dimensions and physical parameters of the PBR unit and an open pond.

In the case of the open pond, the illuminated surface is equal to the ground occupied surface, while in the novel PBR, the illuminated surface to occupied surface ratio is 11, complying with the recommendations for PBR designing given by Posten et a., 2009 [21]. Furthermore, in the present design the occupied surface to culture volume ratio is 4.3 times higher than in the open pond.

Biomass concentration should be also optimized since it determines the optical length of the light through the culture. At very low concentrations (<0.2 kg m^{-3}) near the whole volume remains illuminated, however this too low concentration will predictably result in a low areal or volumetric productivity. Above a concentration of 0.5 kg m^{-3}, the illuminated distance from the irradiated surface is short and near constant. According to the proposed kinetics, above that concentration areal or volumetric productivity do not increase anymore, and even begin to decrease very slowly. However, working at high concentration is more beneficial for downstream processing.

3.2. Hourly and seasonal variations in biomass productivity

The daily areal biomass productivity for three different scenarios was modelled in a PBR unit with D=0.3 m, φ=5º and 1 kg m^{-3} biomass concentration. The three scenarios are: the most favorable one through the year (July daily average), the most unfavorable one (January daily average) and an average day through the whole year, all of them under monthly average cloud cover. In July the reactor receives light during 14.5 hours per day, while in January it is only exposed to sunlight during 8.5 hours. Results of areal productivity (g m^{-2} d^{-1}) along the day are represented in Figure 7. The overall daily productivity, the average productivity during light hours, the photosynthetic efficiency and the biomass yield for a whole day are shown in Table 4.

Scenario	Daily areal productivity (g $m^{-2}d^{-1}$)		Average productivity during light hours (g $m^{-2}d^{-1}$)		Photosynthetic efficiency (%)		Biomass yield (g biomass/mol PAR photons)	
January	15.17	5.74	42.83	15.75	8.75	3.31	0.76	0.29
July	34.57	12.09	56.25	19.67	7.73	2.70	0.67	0.26
Average	26.85	10.08	44.44	16.41	8.30	3.11	0.72	0.27

Table 4. Daily areal productivity (g $m^{-2}d^{-1}$), average productivity during light hours (g $m^{-2}d^{-1}$), photosynthetic efficiency and biomass yield for the three scenarios in the PBR (left) and the open pond (right).

Regarding the daily areal productivity in the PBR, considerable differences can be appreciated between the most favorable and the most unfavorable situations in the year. The productivity on an average day is higher than the average of the two other situations. Since models based on local light intensities and local growth rates tend to under-predict the productivity [10,28], higher values of areal or volumetric productivity may be expected.

Photosynthetic efficiency values are in the range of reported data [35]. Biomass yield are similar to results referred to enclosed PBR [36,37]. Both photosynthetic efficiency and biomass yield are higher in January than in July, which along with the plateau in the upper part of the daily areal productivity curve for July suggest that some photosaturation is taking place during the summer days.

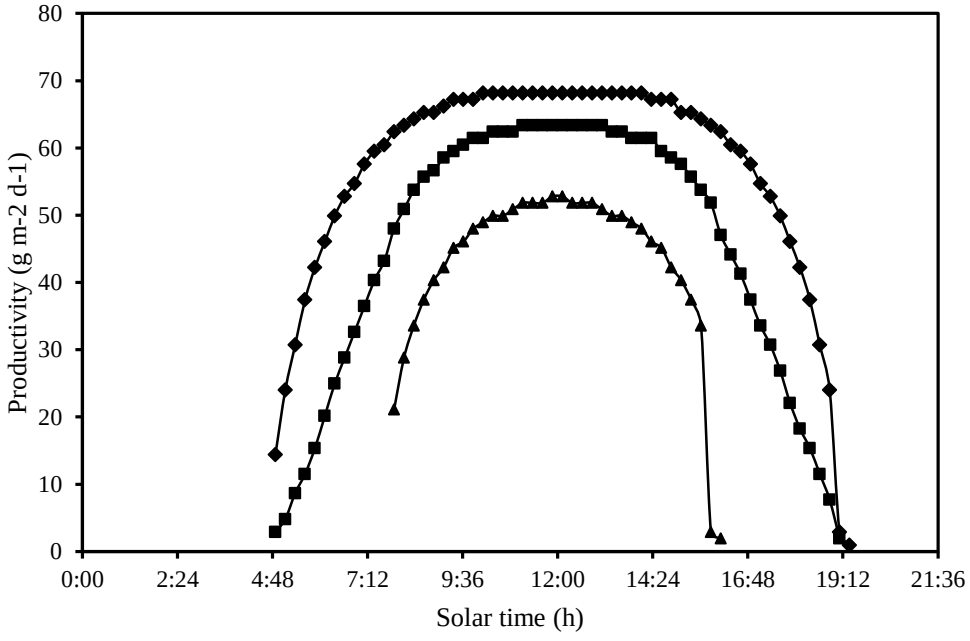

Figure 7. Daily areal productivity (g m^{-2} d^{-1}) for the three different scenarios (▲most unfavorable month, ♦ most favorable month, ■ average month).

Optimizing the cone properties in mid-latitudes, where quite different Sun paths occur during the year, leads to limit the productivity in some part of the year. If the cone is optimized for summer conditions, a high dilution effect would compromise productivity during the winter. On the contrary, if winter conditions are used for optimization, high photosaturation will continue to occur during the summer. In this case, optimization has been carried out for an average day of the year, then some photosaturation takes place during summer time and some excessive dilution effect compromise productivity during the winter. The predicted daily areal productivity for the three scenarios are, in average, 2.72 times higher in the novel PBR than in the open pond.

For comparison, results of other outdoor large scale pilot plants together with the results of this modelling, are included in Table 5.

PBR type	**Daily areal productivity (g $m^{-2}d^{-1}$)**	**Location**	**Reference**
Paddle-wheels open pond	2 - 13.95	Southern Spain	Jimenez et al., 2003[38]
Open Raceway Pond	9.7	The Netherlands	De Vree et al., 2015[39]
Horizontal Tubular PBR	12.1	The Netherlands	De Vree et al., 2015[39]
Vertical Tubular PBR	19.4	The Netherlands	De Vree et al., 2015[39]
Vertical Flat Planel	20.5	The Netherlands	De Vree et al., 2015[39]
High Rate Open Pond	5.5 – 10.2	Southern Spain	Arbib et al., 2017 [40]
Vertical tubular	15.4	Southern Spain	San Pedro et al., [41]
Open Pond	10.08	Northern Spain	This modelling
Novel Deep PBR	26.85	Northern Spain	This modelling

Table 5. Average areal productivities (g $m^{-2}d^{-1}$) of different types of outdoor large scale pilot plants.

3.3. PBR scale-up

As stated before, the situation of the pivot joint as well as the maximum inclination angle of the cones are two main decision variables in the optimization of the cones distribution.

The working illuminated volume per cone and per unit surface were calculated for the two border cases: pivot joint in the apex and in the base. The maximum α is 70º, which is the maximum solar elevation that takes the Sun in the latitude of this case study. Since the characteristics of the cone

and therefore the variation of the water level depend on its maximum tilt angle, three cases were simulated: α_{min} = 20º, 35º and 50º for a cone with a diameter of 0.2 m at the height of the water level when it is in vertical position.

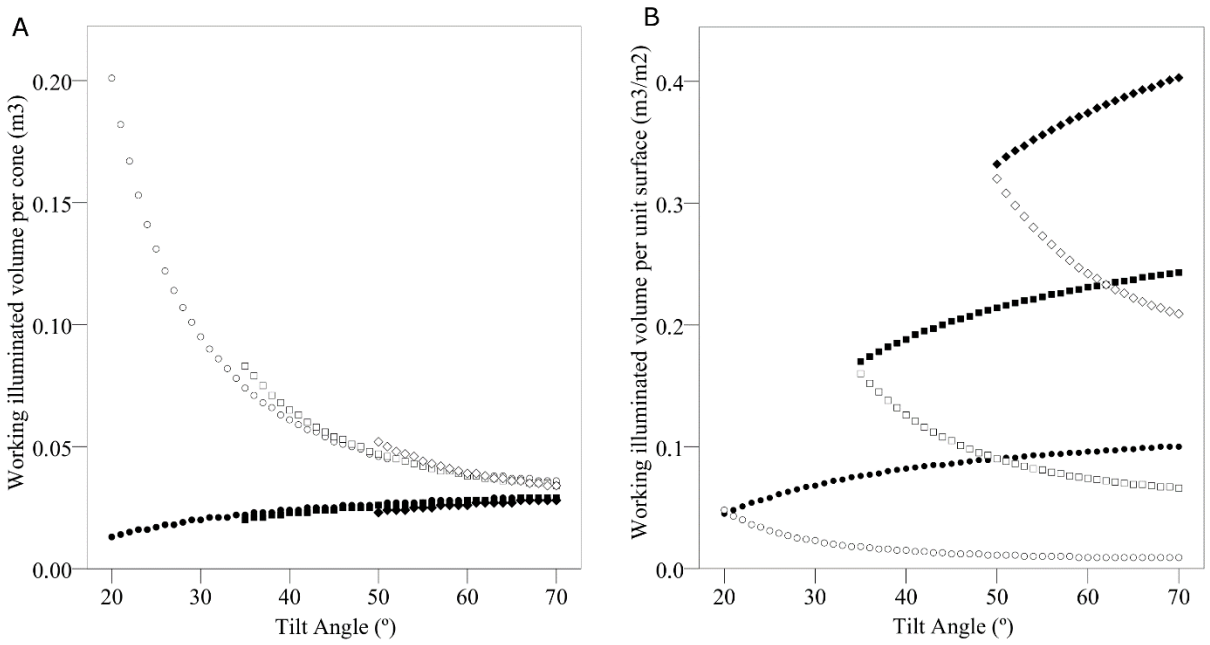

Figure 8. **A**. Variation of the working illuminated volume per PBR unit with the tilt angle, for different situations of the pivot joint and different maximum tilt angle. **B**. Variation of the working illuminated volume per unit surface with the tilt angle, for different situations of the pivot joint and different maximum tilt angle (♦) 50º; (■) 35º; (●) 20º. Filled symbols mean pivot joint in the base while white symbols mean pivot join in the apex.

As shown in Figure 8, placing the pivot joint in the apex results in a high illuminated working volume per cone but a low illuminated volume per unit surface. This is due to the large *Q*, which makes the cones to be very distant one to each other. In the opposite case, when the pivot joint is in the base, *Q* takes its minimum value and the highest number of cones per unit surface is reached. This results in a high illuminated working volume and, as a consequence, in a low ratio dark volume to illuminated volume. As the height of the pivot joint along the axis of the cone decreases, *Q* is larger with respect to the situation in the base, and therefore the number of cones falls. However, the illuminated volume per cone is increased, but not enough to counteract the

decrease of the number of cones. The optimum situation for the pivot joint is the base of the cones since it provides the highest illuminated working volume per unit surface and the lowest dark volume to illuminated volume ratio.

With the pivot joint in the base of the cones, several cones distributions were compared. In all the cases φ took the value of 5º and the cones had fixed margin –*q*– of 0.10 m between the water level and *Q*.

Firstly two base diameters were compared for distributions in which the maximum inclination angle in the South direction is 25º. Although PBR units with larger cones (D=0.3 m) have higher illuminated volume through the year, its value is lower when it is referred to the occupied ground surface. Larger cones provide larger illuminated volumes, but fewer cones can be installed per unit surface. Cones with lower base diameter (D=0.2 m) provide a higher illuminated volume per unit surface through the year. This is represented in Figure 9. Both diameters show a similar pattern in the variation of the illuminated volume-time per unit surface and per year with the angle β, presenting the maximum value when β=45º.

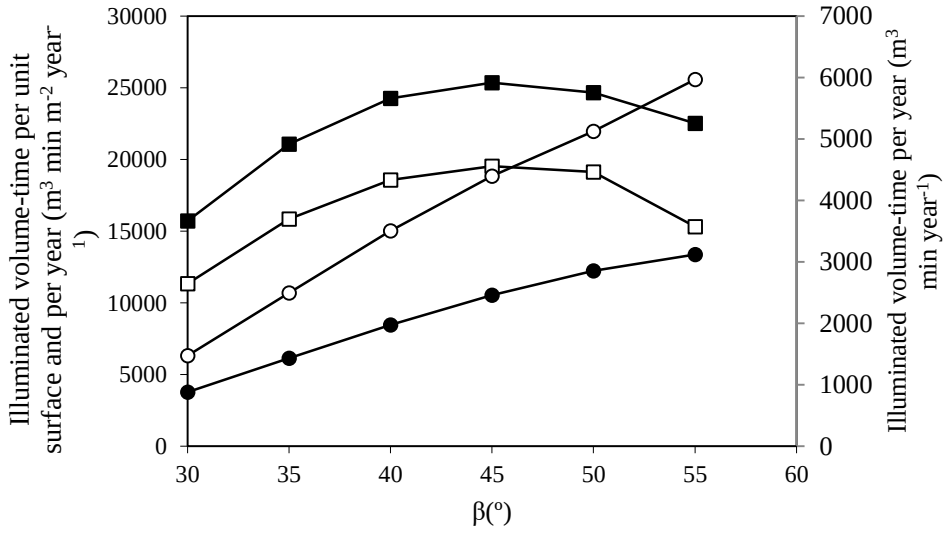

Figure 9. Variation of the illuminated volume-time per unit surface and per year (m^3 min m^{-2} $year^{-1}$) and the illuminated volume-time per year (m^3 min $year^{-1}$) on the cones distribution. In all cases α_S is 25º, and the abscissa axis represents β: (■) m^3 min m^{-2} $year^{-1}$ for a PBR unit with a cone with diameter of 0.2 m at the height of the water level; (□) m^3 min m^{-2} $year^{-1}$ for 0.3 m of diameter; (●) m^3 min $year^{-1}$ for 0.2 m of diameter; (○) m^3 min $year^{-1}$ for 0.3 m of diameter

According to these results, the diameter of 0.2 m seems to result in higher photonic efficiency. Then, several cones distributions where compared for a cone with this diameter. As can be observed in Figure 10, the results of the simulations show that the highest illuminated volume-time per unit surface and per year occur for α_S of 25º and β being 45º.

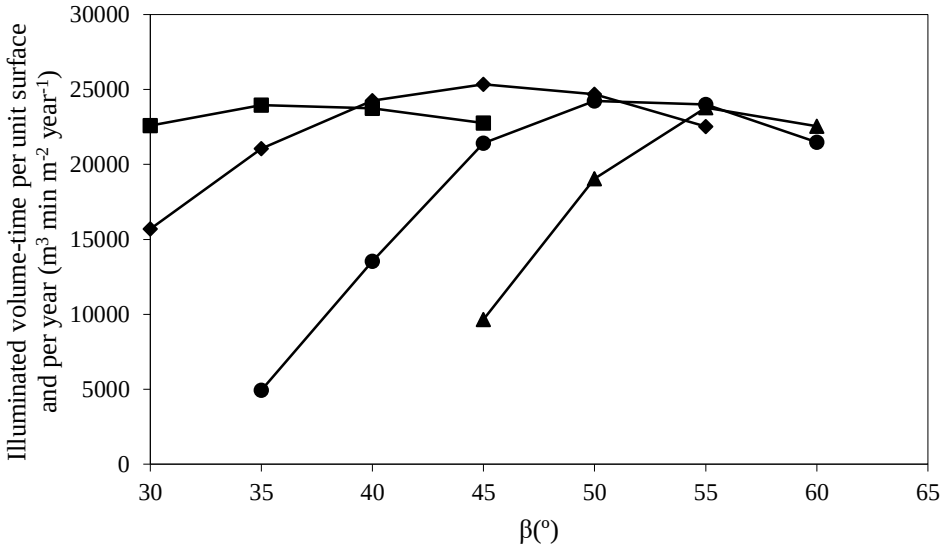

Figure 10. Variation of the illuminated volume-time per unit surface and per year (m^3 min m^{-2} $year^{-1}$) on the cones distribution for a PBR unit with a cone with diameter of 0.2 m at the height of the water level and different α_S: (■) 20; (♦) 25; (●) 30; (▲) 35.

This configuration comprises 13 cones per square meter and makes a regular rhomboid grid with diagonals of 0.47 m. It allows for the caption perpendicularly to the base of the cones of the 67% of the direct radiation falling over the PBR unit. In Figure 11, the angle that limits the inclination of the cone for each Az is represented, considering that 0º is the South direction. There is a first straight part which belongs to the central hours of the day where the inclination is not limited,

since the lowest solar altitude in Santander in the South direction is 25º and this configuration allows the cones to tilt to this angle. The second part represents the angles limited by the cone which is located 45º to the South-West or to the South-East and with a separation of 0.23 m from the studied cone. The third part is the limitation by the cone situated 90º to the West or to the East.

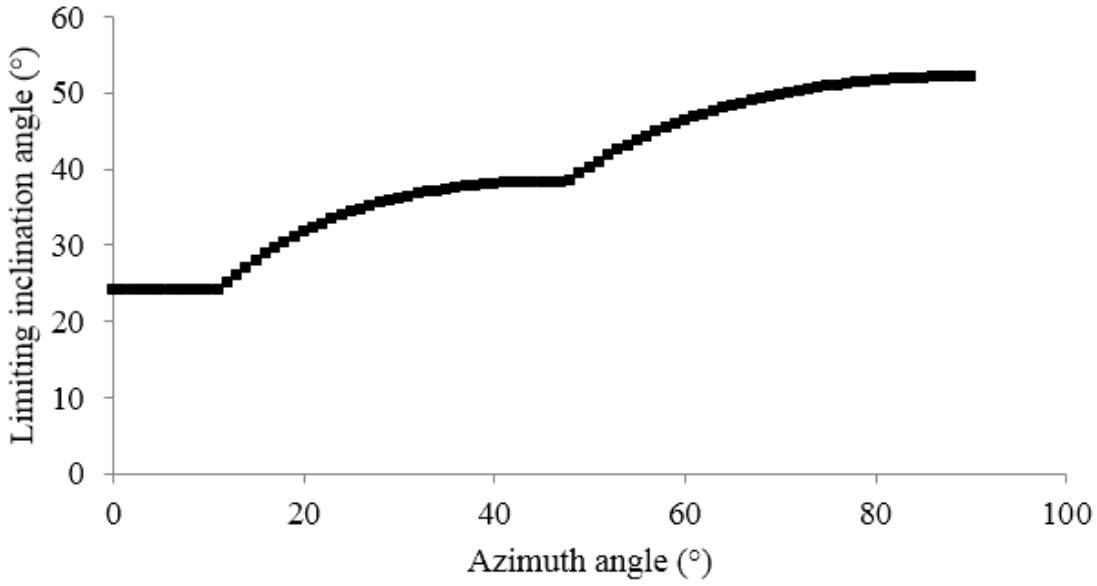

Figure 11. Limiting inclination angle for each Az in a distribution with α_S of 25º and β being 45º

However, several situations provide similar results. Then, another parameter should be used to evaluate the efficiency of those distributions. Since different situations allow for the introduction of a higher or a lower number of cones, they present different dark to illuminate volume ratios. Among the cases represented in Figure 9 that provide the highest illuminated volumes-time per unit surface and per year (>23,000 m^3 min m^{-2} $year^{-1}$), dark to illuminate volume ratios are between 6 and 11. Furthermore, the lowest ratios are due to the presence of a higher number of cones, thus a higher number of smaller dark volumes are placed among the cones, making the alternation between light and dark areas more frequent. Until the date, there is not a clear agreement on how the flashing light affects the microalgae growth although it seems that in

general it is accepted that intermittent illumination enhances photosynthesis [42][43][44]. However, the duration of the L:D cycles do not depend only on the size of light and dark volumes, but also on the agitation and mixing grade.

The distribution that provides the lowest dark to illuminated volume ratio among those having a high illuminated volumes-time per unit surface and per year (>23,000 m^3 min m^{-2} $year^{-1}$) allows the cones to tilt until 25º in South direction and has a β angle of 40º. According to these results, it can be deduced that configurations that limit the cones inclination in South direction cause notable energy losses.

4. Conclusions

A mathematical model of the novel deep PBR was built and its areal productivity was simulated. While conventional PBR exposed to solar light usually receive an excessive amount of energy in the external layers of the culture, the PBR presented hereby takes advantage of the energy in excess distributing it over a higher surface, thus minimizing the photoinhibition and increasing the culture illuminated volume per occupied surface. A unit of volume of the novel PBR was compared with a conventional open pond, showing that it multiplies by 11 the illuminated to occupied surface ratio and reach more than double the yearly average areal biomass productivity. Hence, the novel configuration is highly efficient in land use, providing a low surface requirement solution.

In a mid-latitude location, the longer is the duration of the day and the higher is the irradiance, the greater is the productivity increase with the present PBR configuration. In addition, the illuminated volume through the year per unit surface is increased when the solar altitude along the day is high, thus suggesting that low latitudes are the most appropriate for this design. A procedure to optimize decision variables when scaling-up the PBR, being the situation of the pivot joint of the cones, the maximum inclination angle and the relative position of the cones was

developed, providing a tool for further assessment and specific applications design of the novel PBR.

Authors' contributions

Maria Castrillo took part in the conception of the design, performed the modeling and results analysis and wrote the article. Rubén Díez Montero contributed to the conception of the design and the model and gave critical revisions of the article. Iñaki Tejero is the chief of the research group; he proposed the main idea, supervised the work and gave final approval for submitting the article.

5. References

[1] T.M. Mata, A.A. Martins, N.S. Caetano, Microalgae for biodiesel production and other applications: A review, Renewable and Sustainable Energy Reviews. 14 (2010) 217-232; doi: 10.1016/j.rser.2009.07.020.

[2] N. Norsker, M.J. Barbosa, M.H. Vermue, R.H. Wijffels, Microalgal production - A close look at the economics, Biotechnol. Adv. 29 (2011) 24-27; doi: 10.1016/j.biotechadv.2010.08.005.

[3] Y. Wang, S.-. Ho, C.-. Cheng, W.-. Guo, D. Nagarajan, N.-. Ren, D.-. Lee, J.-. Chang, Perspectives on the feasibility of using microalgae for industrial wastewater treatment, Bioresour. Technol. 222 (2016) 485-497; doi: 10.1016/j.biortech.2016.09.106.

[4] M. Cuaresma, M. Janssen, C. Vílchez, R.H. Wijffels, Horizontal or vertical photobioreactors? How to improve microalgae photosynthetic efficiency, Bioresour. Technol. 102 (2011) 5129-5137; doi: 10.1016/j.biortech.2011.01.078.

[5] M. Janssen, J. Tramper, L.R. Mur, R.H. Wijffels, Enclosed outdoor photobioreactors: Light regime, photosynthetic efficiency, scale-up, and future prospects, Biotechnol. Bioeng. 81 (2003) 193-210; doi: 10.1002/bit.10468.

[6] C.U. Ugwu, H. Aoyagi, H. Uchiyama, Photobioreactors for mass cultivation of algae, Bioresour. Technol. 99 (2008) 4021-4028; doi: 10.1016/j.biortech.2007.01.046.

[7] I. Fernández, F.G. Acién, J.L. Guzmán, M. Berenguel, J.L. Mendoza, Dynamic model of an industrial raceway reactor for microalgae production, Algal Res. 17 (2016) 67-78; doi: 10.1016/j.algal.2016.04.021.

[8] J.C. Ogbonna, H. Yada, H. Masui, H. Tanaka, A novel internally illuminated stirred tank photobioreactor for large- scale cultivation of photosynthetic cells, J. Ferment. Bioeng. 82 (1996) 61-67; doi: 10.1016/0922-338X(96)89456-6.

[9] J.-. Cornet, Calculation of optimal design and ideal productivities of volumetrically lightened photobioreactors using the constructal approach, Chemical Engineering Science. 65 (2010) 985-998; doi: 10.1016/j.ces.2009.09.052.

[10] J.C. Ogbonna, H. Tanaka, Light requirement and photosynthetic cell cultivation - Development of processes for efficient light utilization in photobioreactors, J. Appl. Phycol. 12 (2000) 207-218. doi: https://doi.org/10.1023/A:1008194627239

[11] J. Hu, T. Sato, A photobioreactor for microalgae cultivation with internal illumination considering flashing light effect and optimized light-source arrangement, Energy Conversion and Management. 133 (2017) 558-565; doi: https://doi.org/10.1016/j.enconman.2016.11.008.

[12] R.H. Wijffels, M.J. Barbosa, An outlook on microalgal biofuels, Science. 329 (2010) 796-799; doi: 10.1126/science.1189003.

[13] J.C. Ogbonna, T. Soejima, H. Tanaka, An integrated solar and artificial light system for internal illumination of photobioreactors, J. Biotechnol. 70 (1999) 289-297; doi: 10.1016/S0168-1656(99)00081-4.

[14] J.-. An, B.-. Kim, Biological desulfurization in an optical-fiber photobioreactor using an automatic sunlight collection system, J. Biotechnol. 80 (2000) 35-44; doi: 10.1016/S0168-1656(00)00235-2.

[15] S. Xue, Q. Zhang, X. Wu, C. Yan, W. Cong, A novel photobioreactor structure using optical fibers as inner light source to fulfill flashing light effects of microalgae, Bioresource Technology. 138 (2013) 141-147; doi: 10.1016/j.biortech.2013.03.156

[16] J.-.F. Zijffers, M. Janssen, J. Tramper, R.H. Wijffels, Design process of an area-efficient photobioreactor, Marine Biotechnology. 10 (2008) 404-415; doi: 10.1007/s10126-007-9077-2.

[17] J.-.F. Zijffers, S. Salim, M. Janssen, J. Tramper, R.H. Wijffels, Capturing sunlight into a photobioreactor: Ray tracing simulations of the propagation of light from capture to distribution into the reactor, Chem. Eng. J. 145 (2008) 316-327; doi: 10.1016/j.cej.2008.08.011.

[18] C.H. Hsieh, W.T. Wu, A novel photobioreactor with transparent rectangular chambers for cultivation of microalgae, Biochem. Eng. J. 46 (2009) 300-305; doi: 10.1016/j.bej.2009.06.004.

[19] Evers E.G., A Model for Light-Limited Continuous Cultures: Growth, Shading, and Maintenance, Biotechnology and bioengineering. 38 (1991) 254-259; doi: 10.1002/bit.260380307.

[20] M. Morweiser, O. Kruse, B. Hankamer, C. Posten, Developments and perspectives of photobioreactors for biofuel production, Appl. Microbiol. Biotechnol. 87 (2010) 1291-1301; doi: 10.1007/s00253-010-2697-x.

[21] C. Posten, Design principles of photo-bioreactors for cultivation of microalgae, Eng. Life Sci. 9 (2009) 165-177; doi: 10.1002/elsc.200900003.

[22] S. Hindersin, M. Leupold, M. Kerner, D. Hanelt, Irradiance optimization of outdoor microalgal cultures using solar tracked photobioreactors, Bioprocess and Biosystems Engineering. 36 (2013) 345-355; doi: 10.1007/s00449-012-0790-5.

[23] H. Qiang, D. Faiman, A. Richmond, Optimal tilt angles of enclosed reactors for growing photoautotrophic microorganisms outdoors, J. Ferment. Bioeng. 85 (1998) 230-236; doi: 10.1016/S0922-338X(97)86773-6.

[24] P.M. Slegers, R.H. Wijffels, G. van Straten, A.J.B. van Boxtel, Design scenarios for flat panel photobioreactors, Appl. Energy. 88 (2011) 3342-3353; doi: 10.1016/j.apenergy.2010.12.037.

[25] A.E. Rabe, R.J. Benoit, Mean light intensity: a useful concept in correlating growth rates of dense cultures of microalgae, Biotechnol. Bioeng. 4 (1962) 377-390; doi: 10.1002/bit.260040404.

[26] F.G. Acién Fernández, F. García Camacho, J.A. Sánchez Pérez, J.M. Fernández Sevilla, E. Molina Grima, A model for light distribution and average solar irradiance inside outdoor tubular photobioreactors for the microalgal mass culture, Biotechnol. Bioeng. 55 (1997) 701-714; doi: 10.1002/(SICI)1097-0290(19970905)55:5<701::AID-BIT1>3.0.CO;2-F.

[27] Y.S. Yun, J.M. Park, Kinetic modeling of the light-dependent photosynthetic activity of the green microalga Chlorella vulgaris, Biotechnol. Bioeng. 83 (2003) 303-311; doi: 10.1002/bit.10669.

[28] R. Bosma, E. van Zessen, J.h.H. Reith, J. Tramper, R.H. Wijffels, Prediction of volumetric productivity of an outdoor photobioreactor, Biotechnol. Bioeng. 97 (2007) 1108-1120; doi: 10.1002/bit.21319.

[29] Tejero, J.I.,Castrillo, M., Diez, R., Moreno-Ventas, X.E., Fotobiorreactor para el cultivo de organismos fotótrofos, WO2012072837 A1 (2011).

[30] L.M. Lucas-Salas, M. Castrillo, D. Martinez, Effects of dilution rate and water reuse on biomass and lipid production of Scenedesmus obliquus in a two-stage novel photobioreactor, Bioresour. Technol. 143 (2013) 344-352; doi: 10.1016/j.biortech.2013.06.007.

[31] European Commission, Joint Research Centre Institute for Energy, Renewable Energy Unit, Photovoltaic Geographical Information System (PVGIS), http://re.jrc.ec.europa.eu/pvgis/.2009 (2012).

[32] J.F. Cornet, Calculation of optimal design and ideal productivities of volumetrically lightened photobioreactors using the constructal approach, Chemical Engineering Science. 65 (2010) 985-998; doi: https://doi.org/10.1016/j.ces.2009.09.052

[33] E. Molina Grima, F.G.A. Fernández, F. García Camacho, Y. Chisti, Photobioreactors: Light regime, mass transfer, and scaleup, J. Biotechnol. 70 (1999) 231-247; doi: 10.1016/S0079-6352(99)80118-0.

[34] F. García Camacho, A. Contreras Gómez, F.G. Acién Fernández, J. Fernández Sevilla, E. Molina Grima, Use of concentric-tube airlift photobioreactors for microalgal outdoor mass cultures, Enzyme Microb. Technol. 24 (1999) 164-172; doi: 10.1016/S0141-0229(98)00103-3.

[35] A. Melis, Solar energy conversion efficiencies in photosynthesis: Minimizing the chlorophyll antennae to maximize efficiency, Plant Science. 177 (2009) 272-280; doi:10.1016/j.plantsci.2009.06.005.

[36] M. Cuaresma, M. Janssen, C. Vilchez, R.H. Wijffels, Productivity of Chlorella sorokiniana in a Short Light-Path (SLP) Panel Photobioreactor Under High Irradiance, Biotechnol. Bioeng. 104 (2009) 352-359; doi:10.1002/bit.22394.

[37] R. A., Handbook of Microalgal Culture: Biotechnology and Applied Phycology, John Wiley & Sons, 2008.

[38] C. Jimenez, B.R. Cossio, F.X. Niell, Relationship between physicochemical variables and productivity in open ponds for the production of Spirulina: a predictive model of algal yield, Aquaculture. 221 (2003) 331-345; doi: 10.1016/S0044-8486(03)00123-6.

[39] J. H. de Vree, R. Bosma, M. Janssen, M.J. Barbosa, R. H. Wiljffels. Comparison of four outdoor pilot-scale photobioreactors. Biotechnol. Biofuels. 8:215 (2015); doi: 10.1186/s13068-015-0400-2

[40] Z. Arbib, I. de Godos, J. Ruiz, J. A. Perales. Optimization of pilot high rate algal ponds for simultaneous nutrient removal and lipids production. Sci Total Environ. 589 (2017) 66–72; doi: 10.1016/j.scitotenv.2017.02.206

[41] San Pedro A, et al. Outdoor pilot-scale production of Nannochloropsis gaditana: influence of culture parameters and lipid production rates in tubular photobioreactors. Bioresour Technol. 169 (2014) 667–676. doi: https://doi.org/10.1016/j.biortech.2014.07.052[42] J.C. Ogbonna, H. Yada, H. Tanaka, Effect of cell movement by random mixing between the surface and bottom of photobioreactors on algal productivity, J. Ferment. Bioeng. 79 (1995) 152-157; doi:10.1016/0922-338X(95)94083-4.

[42] J.C. Ogbonna, H. Yada, H. Tanaka, Effect of cell movement by random mixing between the surface and bottom of photobioreactors on algal productivity, J. Ferment. Bioeng. 79 (1995) 152-157; doi:10.1016/0922-338X(95)94083-4.

[43] T. Sato, D. Yamada, S. Hirabayashi, Development of virtual photobioreactor for microalgae culture considering turbulent flow and flashing light effect, Energ. Convers. Manage. 51 (2010) 1196-1201; doi:10.1016/j.enconman.2009.12.030.

[44] J.U. Grobbelaar, Upper limits of photosynthetic productivity and problems of scaling, J. Appl. Phycol. 21 (2009) 519-522; doi: 10.1007/s10811-008-9372-y.